

## Spectroscopic, transport, and magnetic results on the $\text{Nd}_{2-x}\text{A}_x^{4+}\text{CuO}_{4-\delta}$ systems ( $A = \text{Ce}$ and $\text{Th}$ )

G. Liang, J. Chen, and M. Croft

*Department of Physics and Astronomy, Rutgers University, Piscataway, New Jersey 08855-0849*

K. V. Ramanujachary and M. Greenblatt

*Department of Chemistry, Rutgers University, New Brunswick, New Jersey 08903*

M. Hegde

*Ceramics Department, Rutgers University, Piscataway, New Jersey 08855-0849*

(Received 24 March 1989)

Structural, spectroscopic, transport, and magnetic results are presented for  $\text{Nd}_{2-x}\text{A}_x^{4+}\text{CuO}_{4-\delta}$  materials with  $A = \text{Ce}$  and  $\text{Th}$ . The structural and spectroscopic results indicate a continuous evolution in properties up to the stability limit of  $x = 0.2$ . In dramatic contrast, the superconducting properties are sharply peaked near  $x = 0.16$  where the system crosses over from semiconducting-to metallic-type behavior.

Heretofore all of the high- $T_c$  superconducting materials have been  $p$ -type materials with hole conduction occurring in  $\text{CuO}_2$  planes.<sup>1-5</sup> The formal valence of Cu in these compounds is +2 with superconductivity being enhanced (or introduced) with chemical substitution that formally increases the  $\text{Cu}^{3+}$  admixture. For example, the base compounds  $\text{La}_{2-x}\text{Sr}_x\text{CuO}_4$  or  $\text{Y}_1\text{Ba}_2\text{Cu}_3\text{O}_{6.5+y}$  have superconductivity stabilized by increasing  $x$  or  $y$  with the formal Cu valence being  $2+x$  and  $2+2y/3$ , respectively. In contrast, Tokura, Takagi, and Uchida<sup>6</sup> have reported the  $n$ -type superconductor  $\text{Nd}_{2-x}\text{Ce}_x\text{CuO}_{4-\delta}$  where  $x = 0.15$  produces a  $T_c = 24$  K (under the proper reducing annealing conditions). With a formally +4 valence for Ce, the formal Cu valence in these materials is  $2-x-2\delta$  and x-ray-absorption spectroscopic (XAS) measurements by Tranquada *et al.*<sup>7</sup> have indeed established the continuous increase in  $\text{Cu}^{1+}$  admixture with increasing  $x$ . The current importance of this  $n$ -type high- $T_c$  material has been underscored by recent theoretical comments,<sup>8,9</sup> which alternately hint at a new superconductivity mechanism or suggest that these materials might provide an anvil upon which some theoretical schemes can be wrought. In view of the novelty and potential importance of this system, it is clearly essential that the empirical character of the superconductivity be parametrized as quickly as possible.

Here we present structural, spectroscopic, transport, and magnetic results on the  $\text{Nd}_{2-x}\text{A}_x\text{CuO}_{4-\delta}$  systems with  $A = \text{Ce}^{4+}$  and  $\text{Th}^{4+}$ . The occurrence of superconductivity is found to be common to both of these quadrivalent substituted systems. While the structural and spectroscopic data indicate continuous evolutions with increasing substitution, we find that the superconductivity is much more singular in character—being optimized over a narrow composition range.

The samples used in this study were prepared as has been described in the literature.<sup>6,7</sup> All the samples were “reduced” by heating under flowing Ar for 14 h at 960 °C. Samples referred to as “slow cooled” were cooled in the

furnace to room temperature at 6 °C/min and those termed “quenched” were cooled rapidly by removal from the furnace (the Ar atmosphere was maintained for both types of samples). Structural measurements were performed using an automated SCINTAG PAD V powder x-ray diffractometer with monochromatized  $\text{CuK}\alpha$  radiation. The lattice parameters were obtained by least-squares fitting of the observed Bragg lines in the  $10^\circ \leq 2\theta \leq 60^\circ$  range. A standard four-probe dc method was used for the resistivity measurements. A superconducting quantum interference device (SQUID) magnetometer was used for the magnetic measurements. The x-ray-absorption method was described previously.<sup>7</sup> Finally, the x-ray photoemission spectroscopy (XPS) measurements were carried out on scraped pellet surfaces using a KRATOS XSAM system.

We have found that  $\text{Nd}_{2-x}\text{A}_x\text{CuO}_4$  materials forming in the same tetragonal  $T'$  phase<sup>6</sup> as  $\text{Nd}_2\text{CuO}_4$  for  $0.0 \leq x \leq 0.2$  is supported by the monotonic decrease of the  $c$  parameter with  $x$  in this range for both  $A = \text{Ce}$  and  $\text{Th}$ . (The  $a$ -lattice parameter is much less sensitive to substitution.) That  $x = 0.2$  is the terminal concentration for the solution is further indicated by the constancy of the  $c$  parameter in mixtures with  $x > 0.2$  and by the growth in intensity of the Bragg lines of a second phase (cubic  $\text{Ce}_{0.75}\text{Nd}_{0.25}\text{O}_{1.875}$  structure<sup>10</sup>) with increasing  $x$  for  $x > 0.2$ . We note that the monotonic decrease of the  $c$ -axis parameter with increasing  $x$  [i.e., from  $c = 12.151$  Å for  $x = 0$  to  $c = 12.039$  Å for  $A = \text{Ce}(x = 0.2)$  and to  $c = 12.087$  Å for  $A = \text{Th}(x = 0.2)$ ] is qualitatively consistent with the smaller ionic radius of  $\text{Ce}^{4+}$  (relative to  $\text{Th}$ ). However, it is also worth noting that the disparity in the perovskite structure ionic radii of  $\text{Ce}^{4+}$  and  $\text{Th}^{4+}$  still would have suggested a more rapid relative compression with Ce substitution.

The x-ray-absorption measurements<sup>7</sup> on the  $\text{Nd}_{2-x}\text{Ce}_x\text{CuO}_{4-\delta}$  system have (1) established that the Ce is in a valence state greater than +3 and hence adds electrons when substituted into the system and (2) found evidence

for a systematic reduction in the Cu valence (i.e., increasing  $\text{Cu}^{1+}$  admixing) with increasing  $x$ . We show in Fig. 1(a), the difference spectra obtained by subtracting the  $\text{Nd}_2\text{CuO}_4$  copper- $K$  edge spectrum from those of the Ce substituted materials. The difference spectrum for the  $\text{Cu}^{1+}$  standard  $\text{Cu}_2\text{O}$  is also shown. In general, the near edge spectra are quite complicated; however, we focus here on the lowest-energy feature associated with  $\text{Cu}^{1+}$ ,  $1s \rightarrow 4p_\pi$  transitions.<sup>7</sup>

The energy of this feature agrees well with the  $\text{Cu}^{1+}$  standard and its continuous enhancement with increasing  $x$  is clear. In the inset of Fig. 1, we plot the peak height of this feature (normalized to the  $\text{Cu}_2\text{O}$  difference spectrum peak height) versus  $x$ . The data in the inset agree (within experimental error) with a linear relation of unity slope. Thus, within this simple measure of  $\text{Cu}^{1+}$  admixture, it appears that one electron is donated to the Cu sites for every Ce atom substituted. This continuous variation in average Cu valence stands in contrast with the sharply peaked superconducting properties discussed below.

In Fig. 1(b), we present  $\text{Cu}(2p_{3/2})$  XPS results which confirm the increase of  $\text{Cu}^{1+}$  in Ce-doped  $\text{Nd}_2\text{CuO}_{4-\delta}$  pressed-powder materials. The increase in the  $\text{Cu}^{1+}$  admixture in the Ce substituted material is clear from the difference spectra (obtained using the  $\text{Nd}_2\text{CuO}_4$  spectra as a  $\text{Cu}^{2+}$  standard) which exhibits a sharp  $\text{Cu}^{1+}$  peak at 932 eV. Similarly, the  $\text{Cu}(2p_{1/2})$  XPS and  $\text{Cu-LVV}$

Auger spectra both indicate  $\text{Cu}^{1+}$  stabilization upon Ce doping.<sup>11</sup> These results qualitatively reinforce our interpretation of the XAS spectra. In view of surface-surface preparation sensitivity of photoemission spectroscopy however, more extensive studies are needed on low-temperature cleaved crystals.

At temperatures above 24 K, all of these Ce and Th substituted materials exhibited magnetic susceptibilities typical of  $\text{Nd}^{3+}$  with a crystalline electric-field moment reduction below 50 K. The high-temperature ( $50 \text{ K} < T < 370 \text{ K}$ ) susceptibility for the  $x=0.075$  sample obeys a Curie-Weiss form  $\chi \approx C/(T+\Theta)$  with  $C=3.014 \text{ emu K/mole}$  and  $\Theta=56 \text{ K}$ . Here the  $C$  value is exactly what is expected for two  $\text{Nd}^{3+}$ ,  $J=9/2$  per formula unit.<sup>11</sup> No evidence for magnetic order was observed in any of the samples studied. In considering the diamagnetic superconducting contribution to the susceptibility, the strong Nd-paramagnetic background must be remembered.

The resistivity of seven samples in the  $A=\text{Ce}$  system and four in the  $A=\text{Th}$  system are shown in Fig. 2. Three characteristic temperatures related to the resistivity results are plotted versus  $x$  in Fig. 3(a):  $T_{ci}$  is the temperature of the initial onset of superconductivity,  $T_{c0}$  is the highest temperature where the resistivity becomes zero, and  $T_{mid}$  denotes the temperature where the resistivity has dropped to one-half of the normal-state (at onset) value. A crucial point to note is that  $T_{ci}$  is essentially independent of  $x$  for both of these systems with  $T_{ci}(\text{Ce}) \approx 24 \text{ K}$  and  $T_{ci}(\text{Th}) \approx 19 \text{ K}$ . Also significant, the  $T_{c0}$  and  $T_{mid}$  results on the more closely spaced composition set of Ce samples clearly indicates that the bulk fraction of superconducting material is an extremely sharply peaked function of concentration. Here zero resistance occurs when a percolating path of superconducting material extends across the sample. Such percolation requires a bulk fraction above a critical threshold, a threshold set partially by the detailed morphological distribution of the superconducting phase. Clearly the bulk fraction rises above this critical threshold only over a narrow range of  $x$ . The conductivity between  $T_{ci}$  and  $T_{c0}$  depends on the detailed morphology of the superconducting tunneling weak-link regions in which the current density exceeds the critical current density. Increasing bulk fraction of superconducting material will clearly enhance the conductivity between  $T_{ci}$  and  $T_{c0}$ , and hence the sharpness of  $T_{mid}$  peak should also mirror the bulk fraction. Referring to the resistivity results on the Ce system (Fig. 2), we wish to note one last important point; namely, that the semiconducting-type upturn in the resistivity (with decreasing  $T$ ) disappears (and metallic behavior onsets) at  $x=0.16$ —where the superconductivity is most prominent.

Direct confirmation that the bulk superconducting fraction sharply peaks near  $x=0.16$  is provided by the diamagnetic susceptibility (in units of the fully superconducting signal  $-1/4\pi$ ) shown in Fig. 3(b). Field-dependent measurements show a sharp reduction in the diamagnetic signal with increasing magnetic field ( $H$ ) even at very low fields.<sup>11</sup> Although our  $H=25 \text{ Oe}$  results are reduced, they nevertheless show the dramatic enhancement in a superconducting fraction close to  $x=0.16$  [Fig. 3(b)]. Selected slow furnace cooled sam-

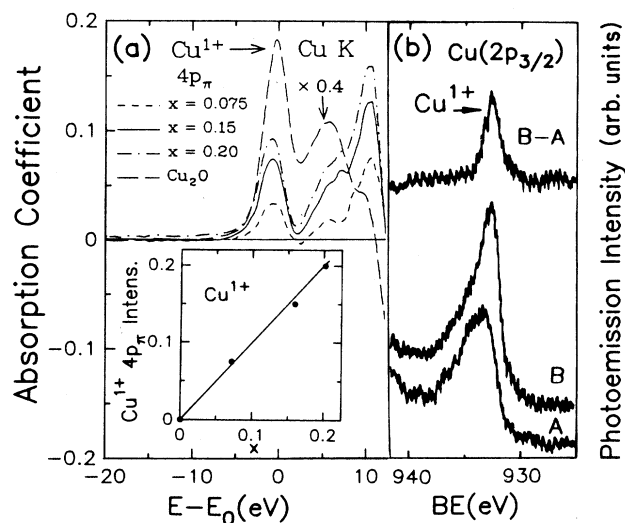


FIG. 1. (a) A differential absorption coefficient spectra at the Cu- $K$  edge for  $\text{Nd}_{2-x}\text{Ce}_x\text{CuO}_{4-\delta}$  compounds. Note that the  $x=0$  spectrum was used as a  $\text{Cu}^{2+}$  standard and was subtracted from all of the  $x > 0$  spectra. Increasing intensity in the  $\text{Cu}^{1+}$   $4p_\pi$  feature in the difference spectra indicates increasing  $\text{Cu}^{1+}$  content. Inset: The peak height of the  $\text{Cu}^{1+}$   $4p_\pi$  spectral feature in the Cu- $K$  edge difference spectra. Here the  $\text{Cu}_2\text{O}$  feature has been used as  $\text{Cu}^{1+}$  standard and all peak heights are normalized to it. (b)  $\text{Cu}(2p_{3/2})$  XPS spectrum of  $\text{Nd}_{2-x}\text{Ce}_x\text{CuO}_{4-\delta}$ ;  $x=0.15$  (spectrum B) and  $x=0.0$  (spectrum A). The difference spectrum (labeled B-A) has a strong  $\text{Cu}^{1+}$  feature at 932 eV confirming the increase of  $\text{Cu}^{1+}$  admixture in the Ce substituted material.

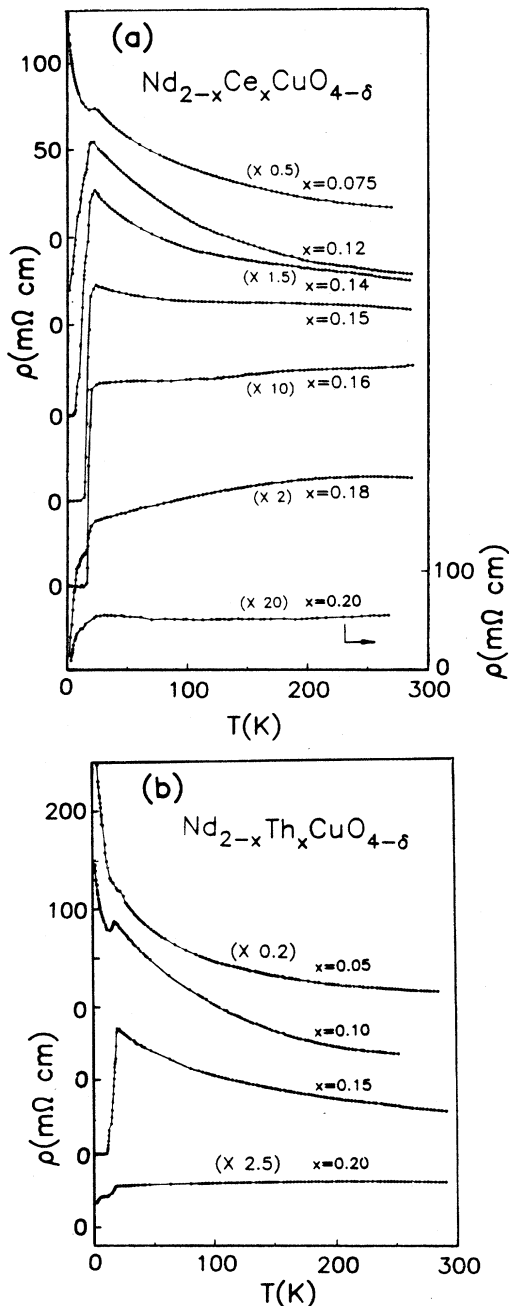


FIG. 2 (a) Resistivity vs  $T$  of the  $\text{Nd}_{2-x}\text{Ce}_x\text{CuO}_{4-\delta}$  system prepared under Ar-annealing (reducing) conditions. The  $x=0.075$  and  $0.20$  samples were cooled slowly and the other samples were quenched. (b) Resistivity vs temperature results for the  $\text{Nd}_{2-x}\text{Th}_x\text{CuO}_{4-\delta}$  system prepared under Ar-annealed (reducing) conditions with slow cooling.

ples show larger superconducting volume fractions than the quenched materials. [This is illustrated by the  $x=0.15$  open circle—data point for the slow-cooled sample in Fig. 3(b).] It should be noted that the presence of diamagnetic contributions to the susceptibility of alloys well removed from  $x=0.16$  can only be discerned via small (field-dependent) reductions in the strong Nd-

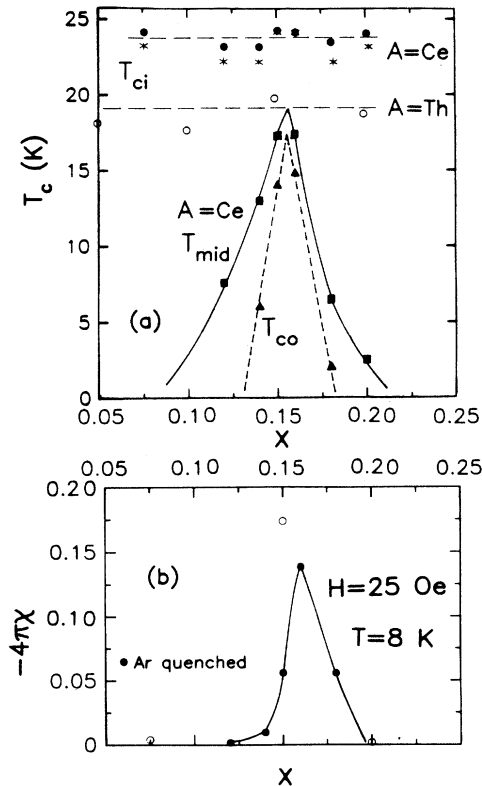


FIG. 3 (a) The locus of resistivity and susceptibility determined superconducting properties in the  $\text{Nd}_{2-x}\text{Ce}_x\text{CuO}_{4-\delta}$  system vs  $x$  for Ar atmosphere annealed (reduced) samples. The initial onset temperature for superconductivity [the first downturn in the resistivity vs  $T$  and the initial diamagnetic signal in  $\chi$  (or  $\chi^{-1}$ ) vs  $T$ ] is plotted as  $\bullet$  and  $\ast$ , respectively. The temperature  $T_{mid}$  is defined as the half-way point ( $R_{onset}/2$ ) in the resistivity drop and is plotted as  $\blacksquare$ . The temperature where the resistivity first reaches zero is denoted  $T_{c0}$  ( $\blacktriangle$ ). The open circles indicate the resistivity determined  $T_{ci}$  for the  $\text{Nd}_{2-x}\text{Th}_x\text{CuO}_{4-\delta}$  system. (b) The diamagnetic fraction  $-4\pi\chi$  vs  $x$  measured in a field of 25 Oe at  $T=8$  K for Ar-quenched sample ( $\bullet$ ) and Ar slowly cooled samples ( $\circ$ ).

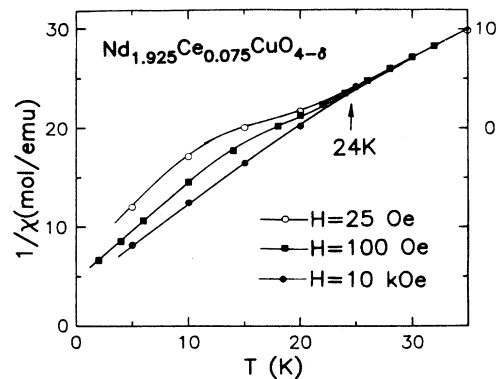


FIG. 4. The inverse susceptibility vs temperature for  $\text{Nd}_{1.925}\text{Ce}_{0.075}\text{CuO}_{4-\delta}$  under a different magnetic field. The curves are normalized to the value of the 100 Oe curve at 30 K. The upturn at  $T \sim 24$  K under low field (25 Oe) indicates the onset of superconductivity.

paramagnetic response. Inverse susceptibility plots, such as shown in Fig. 4 for the  $x=0.075$  sample best illustrate this effect. The diamagnetic signal causes a decrease in  $\chi$  and hence an upturn of the  $\chi^{-1}$  vs  $T$  data. Using this effect we were able to obtain the diamagnetic  $T_{ci}$  for  $A=Ce$  samples well removed from  $x=0.16$ . The diamagnetic onset temperatures  $T_{ci}$ , obtained from  $\chi$  (or  $\chi^{-1}$ ) vs  $T$  data, plotted as \* in Fig. 3(a), lie quite close to the  $T_{ci}$  obtained from the resistivity results.

The picture of superconductivity in the  $A^{4+}$  substituted  $Nd_2CuO_{4-\delta}$  materials which our results support is a singular one. The optimum superconducting composition appears to lie very close to the crossover from semiconducting- to metallic-type conductivity. Superconducting material with a  $T_c$  close to 24 K can, however, be seen in materials with average compositions well away

from  $x=0.16$ . Whether  $A^{4+}$  composition fluctuations (i.e., inhomogeneity of the sample) are responsible here, or whether O-vacancy population fluctuations can stabilize superconductivity over a wider substitution range is at present not clear. Finally, of course, these data raise the question of whether in fact there exists a singular superconducting material with a precise ratio of  $A$  composition to O-vacancy concentration or positional order. More work to clarify this possibility is clearly crucial.

This work was partly supported by the U.S. Office of Naval Research and the National Science Foundation-Solid State Chemistry Grant No. DMR-87-14072 (M.G. and K.V.R.).

<sup>1</sup>J. G. Bednorz and K. A. Müller, *Z. Phys. B* **64**, 189 (1986).

<sup>2</sup>M. K. Wu *et al.*, *Phys. Rev. Lett.* **58**, 908 (1987).

<sup>3</sup>H. Maeda, Y. Tanaka, M. Fukutomi, and T. Asano, *Jpn. J. Appl. Phys.* **27**, L209 (1988).

<sup>4</sup>Z. Z. Sheng and A. M. Hermann, *Nature (London)* **322**, 55 (1988).

<sup>5</sup>For examples, see N. P. Ong *et al.*, *Phys. Rev. B* **35**, 8807 (1987), Z. Z. Wong *et al.*, *ibid.* **36**, 7222 (1987).

<sup>6</sup>Y. Tokura, H. Takagi, and S. Uchida, *Nature (London)* **337**, 345 (1989).

<sup>7</sup>J. Tranquada, S. Heald, A. Moodenbaugh, G. Liang, and M. Croft, *Nature (London)* **337**, 720 (1989).

<sup>8</sup>V. J. Emery, *Nature (London)* **337**, 306 (1989).

<sup>9</sup>T. M. Rice, *Nature (London)* **337**, 689 (1989).

<sup>10</sup>Smith and McCarthy (unpublished).

<sup>11</sup>G. Liang, M. Hegde, J. Chen, and M. Croft (unpublished).